Current Research (2024) Newfoundland and Labrador Department of Industry, Energy and Technology Geological Survey, Report 24-1, pages 79-96

NEW U–Pb AGE CONSTRAINTS ON KEY UNITS WITHIN THE BUCHANS CAMP, SOUTHERN BUCHANS–ROBERTS ARM BELT, CENTRAL NEWFOUNDLAND

G.W. Sparkes and M.A. Hamilton[1]
Mineral Deposits Section
[1]Jack Satterly Geochronology Laboratory, Department of Earth Sciences,
University of Toronto, Toronto, ON, M5S 3B1

ABSTRACT

The geochronology of the Buchans Group clearly demonstrates that most of the formations contained within it were deposited at ca. *470 Ma. An age from the oldest formation, the Lundberg Hill Formation, illustrates that some of the earliest felsic volcanism occurred at 471.11 ± 0.35 Ma. This was followed by the main episode of intermediate to felsic volcanism, which began with the deposition of the Intermediate Footwall member of the Ski Hill Formation at 471.7 ± 0.6 Ma. The transition to felsic-dominated volcanism is marked by the deposition of the Buchans River Formation at 470.20 ± 0.70 Ma. This age also represents the best approximation for the formation of massive sulphide deposits within the Buchans camp, based on current stratigraphic interpretations and geochronological constraints. Felsic volcanism of a similar age to that identified within the Buchans Group is also developed in and around Mary March Brook, where a sample of rhyolite has been dated at 470.09 ± 0.39 Ma.*

The emplacement of post-mineralization felsic dykes within the volcanic stratigraphy of the Buchans camp provide minimum age constraints on the local development of argillic to advanced argillic hydrothermal alteration and subsequent thrust faulting. An age of 467.51 ± 0.44 Ma from a quartz–feldspar-phyric rhyolite dyke from the Tower prospect provides a minimum constraint on the development of hydrothermal alteration attributed to the development of volcanogenic massive sulphide (VMS) mineralization in the area. This mineralization and the related host rocks were subsequently deformed and thrust-imbricated during later deformation. A felsic dyke, which intruded along a significant fault structure known as the Old Buchans Fault, provides an age of 450.32 ± 0.68 Ma, demonstrating that the massive sulphide deposits in the area were being deformed and imbricated by the Late Ordovician.

These geochronological constraints provide valuable new insight into the development and subsequent deformation of an important VMS camp within the regionally extensive Buchans–Roberts Arm Belt. Based on current age constraints, hydrothermal activity within the Buchans camp can be bracketed between 472.3–467.1 Ma, constraining mineralization to a period of some 5.2 Ma. When combined with the recently completed volcanic-facies mapping conducted in the area, the entire dataset illustrates the complexity of the volcanic stratigraphy within the Buchans camp, and highlights the importance of precision chemical abrasion-isotope dilution-thermal ionization mass spectrometry (CA-ID-TIMS) zircon geochronology in deciphering the overall temporal order of these events.

INTRODUCTION

Sampling of key geological units, from both drillcore and outcrop, within the immediate Buchans area and along strike to the northeast, have produced new age constraints on the formation and subsequent deformation of the volcanogenic massive sulphide (VMS) deposits. The current study targeted select units within the southern Buchans–Roberts Arm Belt (BRAB) for chemical abrasion-isotope dilution-thermal ionization mass spectrometry (CA-ID-TIMS) zircon geochronology, to address several key questions. These are: 1) What is the areal extent of the *ca.* 470 Ma volcanic rocks reported by Sparkes *et al.* (2021); 2) What are the age constraints on the development of VMS mineralization and associated alteration, and 3) What is the age of felsic volcanic rocks within the northeastern extent of the southern BRAB, located in the area east of Mary March Brook (Figure 1).

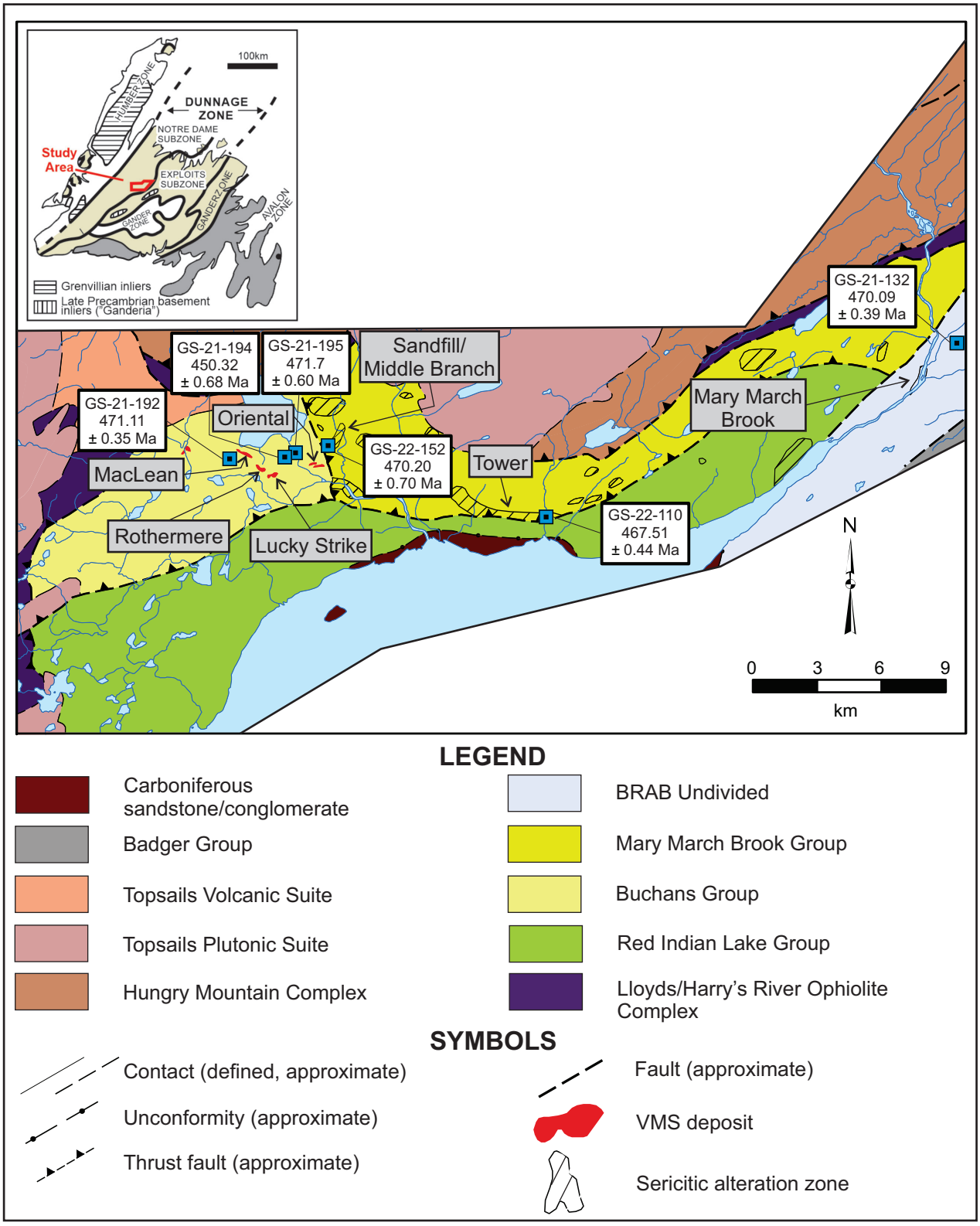

Figure 1. *Regional compilation map outlining the geology and location of geochronological sample sites; geology modified from Zagorevski* et al. *(2015). Note the alteration zones are drawn to encompass drillhole-collar locations that are reported to have intersected white mica alteration at depth. BRAB=Buchans–Roberts Arm Belt. Note that sample GS-22-152 is from drillcore and is projected to surface and represents a sample of the Buchans River Formation within the structural footwall beneath the Mary March Brook group.*

These investigations have demonstrated that the extent of the *ca.* 470 Ma volcanic sequence is more widespread than previously thought, with rocks of this age bracketing much of the Buchans Group. In addition, the development of VMS mineralization and related hydrothermal alteration is now demonstrated to have formed, at least in part, around this time. Finally, the intrusion of post-mineral felsic dykes within the volcanic stratigraphy provides minimum age constraints on the development of localized advanced argillic alteration, inferred to be associated with the development of VMS systems, and the subsequent deformation of these hydrothermal systems. These data combine to highlight a significant period of short-lived felsic volcanism and related VMS mineralization at *ca.* 470 Ma within the southern BRAB, which was subsequently deformed during the Late Ordovician. The age constraints reported here provide new insight into the relative timing of these events within the southern BRAB, and highlight potential correlations with other hydrothermal systems of a similar age, developed farther to the northeast within the central portion of the BRAB (*cf.* Sparkes *et al.*, 2021).

REGIONAL GEOLOGY

The geology of the southern BRAB, primarily confined to the area north of Beothuk Lake (formerly known as Red Indian Lake), has most recently been discussed by Zagorevski and Rogers (2008, 2009), Zagorevski *et al.* (2007, 2015, 2016) and Sparkes *et al.* (2021). The geology of this area has been subdivided into five units, consisting of the Lloyds/Harry's River Ophiolite and Hungry Mountain complexes, and the Mary March Brook, Buchans and the Red Indian Lake groups (Figure 1). The Buchans Group is further subdivided (*see* Thurlow and Swanson, 1987) into the Lundberg Hill, Ski Hill, Buchans River and Sandy Lake formations. The stratigraphy of the Buchans area has recently been modified to include the Intermediate Footwall member of the Ski Hill Formation, and upper and lower members within the Buchans River Formation (*see* Allen *et al.*, *this volume* and references therein). Only the Buchans, Mary March Brook and the Red Indian Lake groups are discussed here in further detail, as they have relevance to the current study.

The Mary March Brook group of Zagorevski and Rogers (2008, 2009), locally, structurally overlies rocks of the Buchans Group, and consists of bimodal tholeiitic and calc-alkalic volcanic rocks. The formation of tholeiitic rhyolite cryptodomes and coeval island-arc tholeiitic basalts were accompanied by the deposition of rare polymictic debris flows and locally developed hydrothermal alteration and VMS mineralization, and are conformably overlain by bimodal calc-alkalic volcanic rocks (Zagorevski and Rogers, 2008, 2009). Rocks from within this group are interpreted to have formed within a back-arc or intra-arc rift setting and have been dated by sensitive high-resolution ion microprobe (SHRIMP) at 461.5 ± 4 Ma (Zagorevski *et al.*, 2016). This group is host to localized VMS mineralization and related alteration zones, which include the Beaver Pond, Seal Pond, Little Sandy, Woodman's Brook and Middle Branch East prospects (*cf.* Sparkes, 2022).

The Buchans Group is composed of calc-alkalic basaltic and rhyolitic rocks of continental-arc affinity, along with characteristic granitoid-bearing conglomerate and debris flows (Thurlow and Swanson, 1987; Swinden *et al.*, 1997; Zagorevski *et al.*, 2015, 2016). SHRIMP dating of volcanic rocks within lower stratigraphic levels of the group range from 465 ± 4 to 463 ± 4 Ma, while a felsic crystal tuff from stratigraphically higher in the sequence is dated at 462 ± 4 Ma (Zagorevski *et al.*, 2015, 2016). Thermal ionization mass spectrometry (TIMS) dating of granitoid clasts from within the debris flows of the Buchans mine area provide an age of 464 ± 4 Ma (Whalen *et al.*, 2013), while CA-ID-TIMS dating of a felsic volcanic rock located stratigraphically below one of the mineralized debris flows at the MacLean deposit provides the oldest age of 471 ± 1.6 Ma (Sparkes *et al.*, 2021). The Buchans Group is well known for its VMS mineralization, which includes the past-producing Oriental, Lucky Strike, Rothermere and MacLean deposits (Figure 1).

The Red Indian Lake Group is composed of tholeiitic mafic, and overlying calc-alkalic bimodal volcanic rocks, with the two sequences locally separated by polymictic conglomerate (Zagorevski *et al.*, 2006; Zagorevski and Rogers, 2008, 2009). Basement rocks are composed of island-arc tholeiities to back-arc basin basalts, along with minor felsic volcanic rocks interpreted to have formed within a rifted arc or back-arc type setting (Zagorevski *et al.*, 2006). Rocks included within the Red Indian Lake Group have produced SHRIMP ages ranging from 465 ± 4 to 462 +2/-9 Ma (Zagorevski *et al.*, 2016) and host several notable VMS occurrences, which include the Mary March and Connell prospects (*cf.* Sparkes, 2022).

Rocks located in the eastern portion of the southern BRAB remain poorly constrained, in part due to poor outcrop exposure (BRAB undivided; Figure 1). Much of the information about this area comes from drillcore, which contains structurally interleaved mafic and felsic volcanic rocks and related volcaniclastic units. Preliminary examination of airborne geophysical data suggests the presence of a significant northeast trending fault structure within the area of Mary March Brook (Figure 1), which locally displays a close spatial association with red sandstone and interbedded

conglomerate of an inferred Carboniferous age. New geochronological data presented here from a felsic unit, intersected in drillcore in the area east of Mary March Brook, supports the inclusion of these felsic volcanic rocks with the *ca.* 470 Ma felsic volcanic rocks of the southern BRAB. However, as to which group these rocks belong to remains uncertain. Regional mapping by Zagorevski *et al.* (2016) correlates these rocks with the Red Indian Lake Group, but immediately to the northeast, the same rocks are correlated with the Gullbridge structural tract by O'Brien (2009; *cf.* Sparkes et al., 2021).

The complex structural geology of the Buchans area has been discussed in numerous reports (*e.g.*, Calon and Green, 1987; Kirkham, 1987; Thurlow and Swanson, 1987; Thurlow *et al.*, 1992). However, the timing of structural events is poorly constrained and has mainly been defined, broadly, as a pre-Topsails Granite (*ca.* 430 Ma; Whalen *et al.*, 1987) event (Thurlow and Swanson, 1987). One important thrust structure identified by previous studies in the Buchans area is the Old Buchans Fault, which forms the floor thrust to the structural panel hosting the Lucky Strike and Rothermere ore bodies (Calon and Green, 1987; Thurlow and Swanson, 1987; Thurlow *et al.*, 1992). Recent detailed logging of diamond-drill core by Buchans Minerals personnel has identified a felsic dyke that intrudes along the Old Buchans Fault northwest of the Oriental deposits. This unit was targeted for geochronological study to constrain the timing of thrust faulting and the related structural dismemberment of massive sulphide deposits of the Buchans camp (*see* below).

LOCAL GEOLOGY

The following summary focuses on providing geological context for the six geochronological samples collected as part of this study. These samples include four from felsic volcanic rocks, three of which are from various units within the Buchans Group stratigraphy, and one from the area of Mary March Brook (Figure 1). In addition, two samples of felsic dykes were collected from drillcore to provide minimum age constraints on the development of hydrothermal alteration and regional tectonics.

BUCHANS AREA

Recent detailed facies mapping within the Buchans area has resulted in minor revisions of the Buchans Group stratigraphy, which includes the introduction of an Intermediate Footwall member within the Ski Hill Formation, and upper and lower members within the Buchans River Formation (Allen *et al.*, *this volume* and references therein; Figure 2). Geochronological sampling in the Buchans area focused on testing the extent of the *ca.* 470 Ma volcanic rocks reported by Sparkes *et al.* (2021). To test the age span within the Buchans Group stratigraphy, a sample was collected from the Lundberg Hill Formation, representing some of the oldest rocks in the area (Figure 2). This sample consisted of fine-grained vitric, diffusely stratified siltstone, inferred to be related to the eruption of a pyroclastic ash, and was collected from drillhole H-2783 (GS-21-192; Figure 3; Plate 1A; Table 1).

Moving up section, a second sample was collected from an outcrop in the area of the Buchans River, representing a sample from the re-introduced Intermediate Footwall member (*cf.* Thurlow and Swanson (1981)) of the Ski Hill Formation (GS-21-195; Figure 2; Plate 2; Table 1). This sample consisted of weakly feldspar-phyric coherent rhyolite (Plate 1B). The collection site is the same locality that was previously sampled for SHRIMP analysis by Zagorevski *et al.* (2016; sample RAX05913), and was collected to test the potential discrepancy between the different dating techniques used in the Buchans area (SHRIMP *vs.* CA-ID-TIMS).

To constrain the timing of VMS mineralization, a third sample was collected from a synvolcanic felsic intrusion bound by ore-clast bearing horizons and thus its age is interpreted, at least in part, to be synchronous with VMS mineralization (GS-22-152; Figure 2; Table 1). This sample was collected from drillhole H-07-3349, and represents a sample of the newly recognized lower member of the Buchans River Formation (Oriental-Sandfill member of Allen *et al.* (*this volume* and references therein)). The sample consisted of massive monomict vitric (± lithic) quartz–feldspar-phyric rhyolite breccia (Plate 1C), which displays a peperitic contact with underlying rhyolite pumice breccia (Figure 4). The latter unit is locally host to massive sulphide clasts and is inferred to postdate VMS mineralization at this stratigraphic level (Allen and Schofield, 2023).

Finally, a felsic dyke that intrudes along the Old Buchans Fault in the area to the northwest of the Oriental deposits was sampled to constrain the age of thrust faulting. The sample consisted of feldspar-phyric rhyolite (GS-21-194; Plate 1D), and was collected from drillhole H-10-3421 (Figure 5; Table 1). The dyke intrudes along the tectonic contact that separates mineralized felsic volcanic rocks of the Buchans River Formation within the hangingwall, from barren siliciclastic rocks of the Sandy Lake Formation within the footwall (Plate 3), representing the floor thrust of the Lucky Strike Duplex (Calon and Green, 1987).

TOWER PROSPECT

The Tower prospect was identified by Sparkes (2022) as an area hosting the local development of advanced argillic alteration (Figure 1). Further study of this area has identified

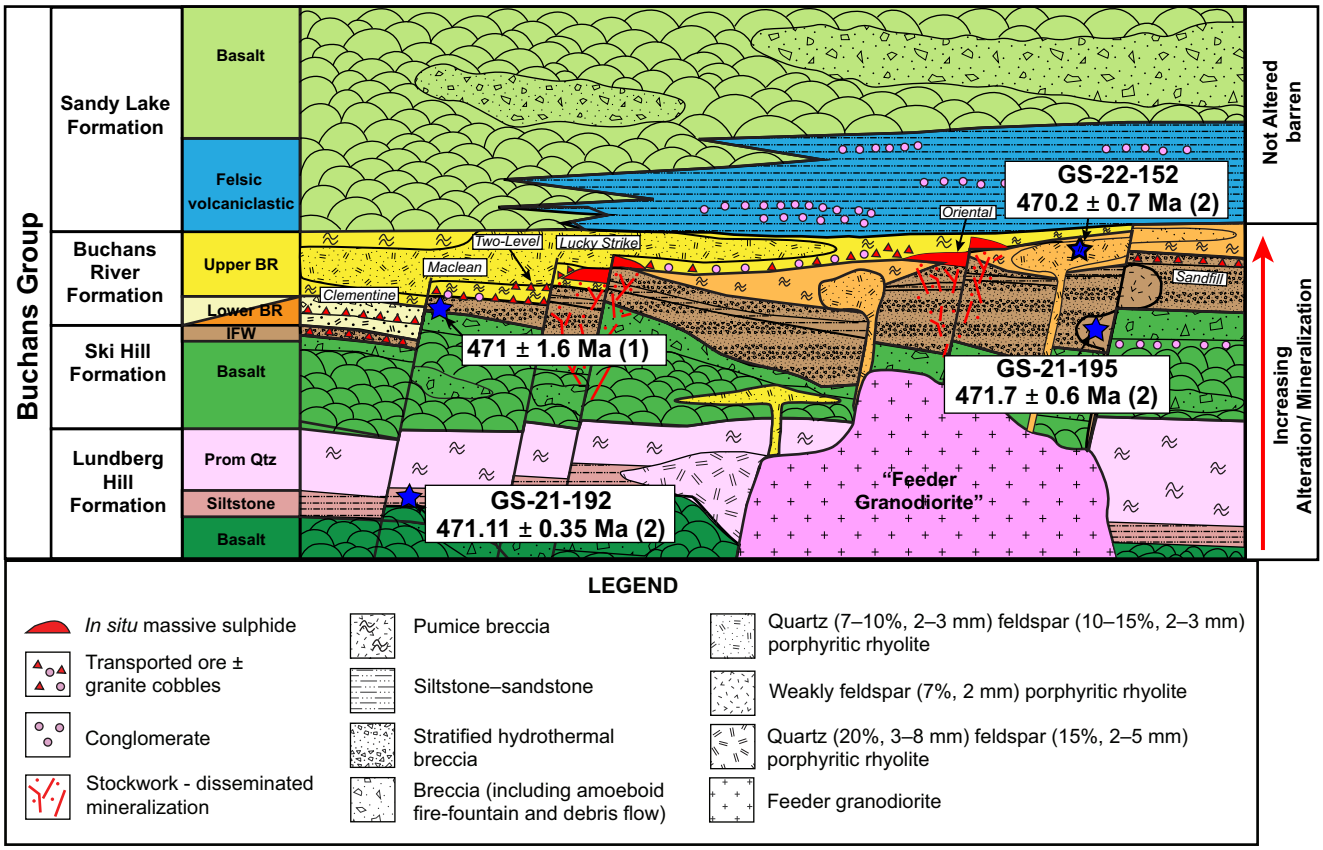

Figure 2. *Revised stratigraphic scheme for the Buchans area (Allen and Schofield, 2023); modified from Thurlow and Swanson (1987). Note the numbers following the compiled geochronology samples (blue stars) represent the data source: (1) Sparkes* et al.*, 2021; (2) this study. Prom Qtz=Prominent quartz unit; IFW=Intermediate Footwall member of the Ski Hill Formation, and the division of the lower Buchans River Formation illustrates the Clementine (light yellow) and Oriental-Sandfill (orange) members.*

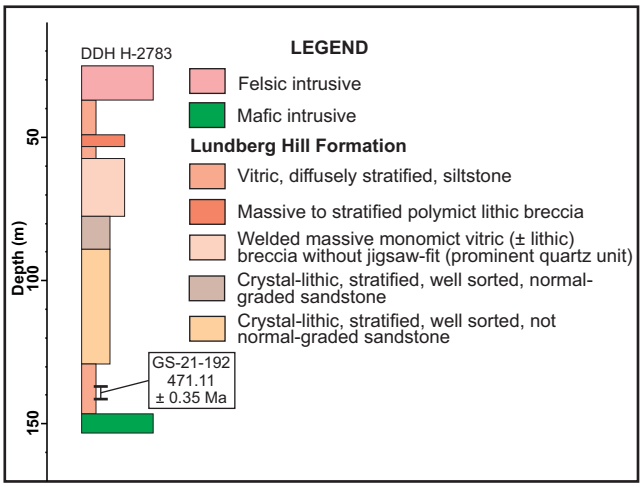

Figure 3. *Partial strip log of DDH H-2783 outlining the distribution of units and the location of the geochronological sample site (GS-21-192).*

similar alteration within a drillhole inferred to intersect the eastern extension of the Tower alteration zone (DDH LS-2K-005; Saunders *et al.*, 2000), which intersected up to 70 m of argillic to advanced argillic alteration hosted with a massive polymict lithic breccia unit (Figure 6; Plate 4A). Short wavelength infrared (SWIR) analysis of this alteration zone indicates the alteration is dominated by paragonite–paragonitic-illite–montmorillonite along with the local development of lesser pyrophyllite, and is bound by iron-chlorite altered mafic volcanic and related volcaniclastic rocks. This stratiform zone of hydrothermal alteration is locally crosscut by a post-alteration quartz–feldspar-phyric rhyolite dyke, which was sampled for geochronological study (GS-22-110; Figure 6; Plate 1E; Table 1). This sample consisted of quartz–feldspar-phyric rhyolite displaying sharp intrusive contacts with the adjacent altered lithic breccia unit (Plate 4B). The dated sample is dominated by iron–magnesium-chlorite and lesser paragonitic-illite, based on SWIR analysis.

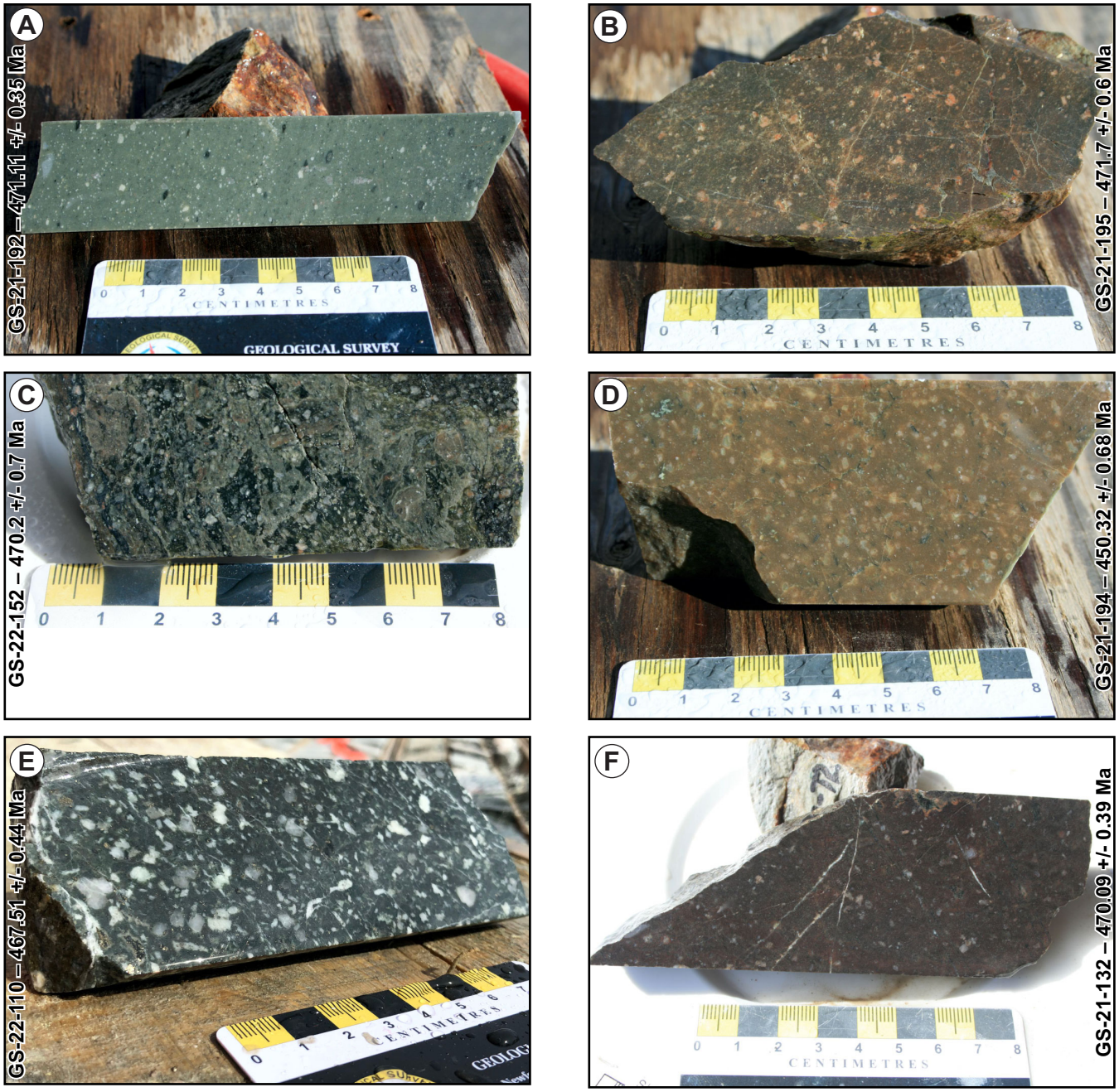

Plate 1. *Representative photographs of each of the samples collected for geochronological study. A) GS-21-192; vitric, diffusely stratified siltstone of the Lundberg Hill Formation, DDH H-2783, between 149.1–155.7 m depth; sample characterized by phengitic white mica alteration; B) GS-21-195; weakly feldspar-phyric coherent rhyolite of the Intermediate Footwall member; sample characterized by siderite–iron-chlorite alteration; C) GS-22-152; massive monomict vitric (± lithic) quartz–feldspar-phyric rhyolite breccia of the lower Buchans River Formation (Oriental-Sandfill member), DDH H-07-3349, between 174.6–177.4 m depth; sample characterized by phengitic illite–magnesium-chlorite alteration; D) GS-21-194; feldspar-phyric rhyolite dyke, DDH H-10-3421, between 383.3–387.6 m depth; E) GS-22-110; quartz–feldspar-phyric rhyolite dyke, DDH LS-2K-005, between 160.5–162.3 m depth; F) GS-21-132; quartz–feldspar-phyric rhyolite, DDH BJ-03-014, between 171.6–175.5 m depth.*

Table 1. Sample location and description data for geochronological samples discussed in text

Sample No.	UTM_E	UTM_N	Datum	Zone	Sample Type	Drillhole	Depth (m)	Rock Type
GS-21-132	542728	5414159	NAD 83	21	Drillcore	BJ-03-014	171.6–175.5	Quartz–feldspar-phyric rhyolite
GS-21-192	507548	5408743	NAD 83	21	Drillcore	H-2783	149.1–155.7	Vitric, diffusely stratified siltstone
GS-21-194	510982	5408683	NAD 83	21	Drillcore	H-10-3421	383.3–387.6	Feldspar-phyric rhyolite
GS-21-195	511065	5408768	NAD 83	21	Outcrop	N/A	N/A	Weakly feldspar-phyric coherent rhyolite
GS-22-110	522271	5406139	NAD 83	21	Drillcore	LS-2K-005	160.5–162.3	Quartz–feldspar-phyric rhyolite dyke
GS-22-152	512072	5409020	NAD 83	21	Drillcore	H-07-3349	174.6–177.4	Massive monomict vitric (± lithic) quartz–feldspar-phyric rhyolite breccia

Plate 2. *Collection site of sample GS-21-195 along the east side of the Buchans River.*

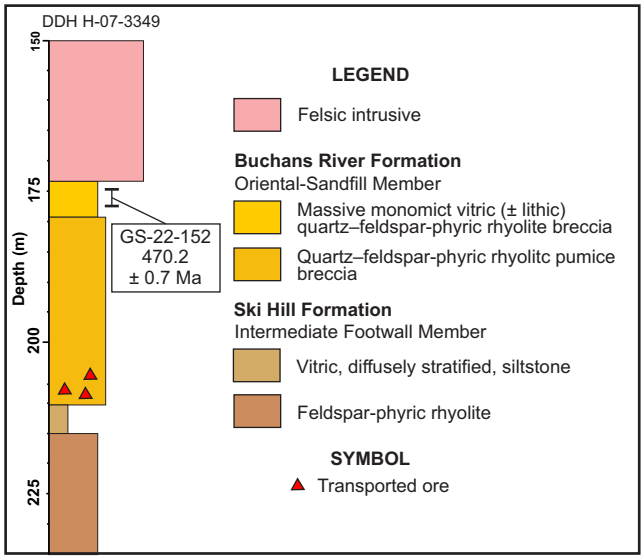

Figure 4. *Partial strip log of DDH H-07-3349 outlining the distribution of units and the location of the geochronological sample site (GS-22-152).*

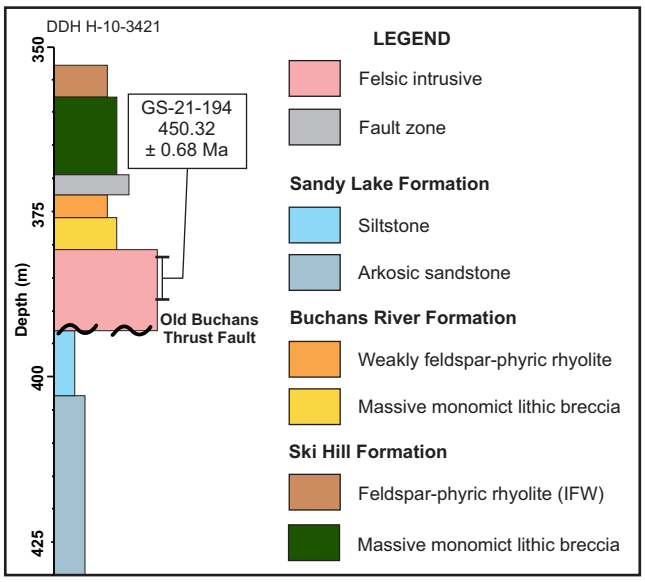

Figure 5. *Partial strip log of DDH H-10-3421 outlining the distribution of units and the location of the geochronological sample site (GS-21-194).*

Plate 3. *Photograph of the dated felsic dyke intruding along the Old Buchans Fault; DDH H-10-3421, 390 m depth. Note the xenolith of the structurally brecciated siltstone to the right of the scale card and the relatively undeformed nature of the felsic dyke* vs. *the underlying siltstone unit.*

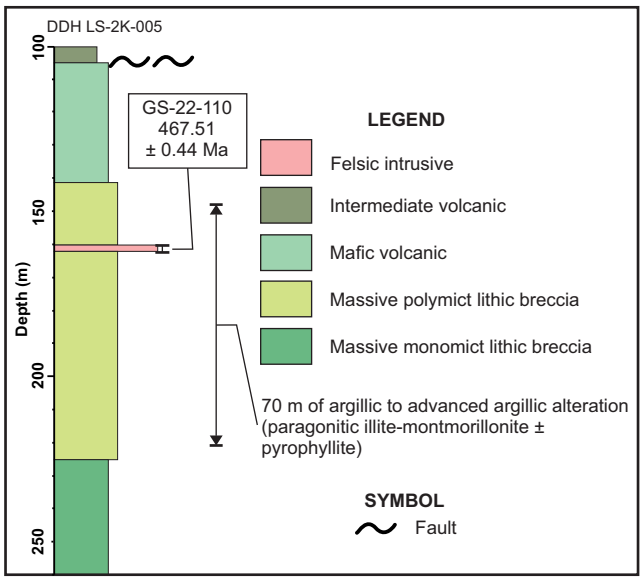

Figure 6. *Partial strip log of DDH LS-2K-005 outlining the distribution of units and the location of the geochronological sample site (GS-22-110).*

MARY MARCH BROOK AREA

Rock units within the Mary March brook area have been correlated both with the Red Indian Lake Group (Zagorevski *et al.*, 2016), as well as the Gullbridge structural tract (O'Brien, 2009; *cf.* Sparkes *et al.*, 2021). Outcrop in the area east of Mary March brook is limited, so much of the geological information gained from this area is gathered from diamond-drill holes. The easternmost drillhole containing felsic volcanic rocks, DDH BJ-03-014, was targeted for geochronological sampling. The upper portion of this drillhole is dominated by a medium-grained gabbroic intrusive unit (Figure 7). Below this intrusion is a quartz–feldspar-phyric rhyolite, which overlies amygdaloidal basalt. The marginal contact zone of the rhyolite displays a well-developed hyaloclastite texture at the contact with the basalt (Plate 5). The sampled material consisted of massive quartz–feldspar-phyric rhyolite (GS-21-132; Plate 1F; Table 1) and is inferred to represent a subaqueous lava or shallow-level intrusion.

U–Pb GEOCHRONOLOGY

Geochronological samples were processed at the Jack Satterly Geochronology Laboratory at the Department of Earth Science, University of Toronto. Sample preparation and procedures followed those outlined in Hamilton *et al.* (2023). The following summary provides a brief petrographic description along with details on the overall zircon recovery and related analyses for each sample. Note all reported errors in the text, figures and Table 2 are presented at the 2-sigma level of uncertainty.

BUCHANS AREA

The sample from the Lundberg Hill Formation (GS-2-21-192) consists of a fine-grained groundmass of quartz hosting rare medium-grained feldspar crystals and patchy carbonate alteration (Plate 6). This sample produced a modest amount of mostly good quality, clear and colourless to pale yellow, short, sharp prismatic grains (Plate 7). In total, 6 fractions were analyzed from this sample. Three of these fractions (Z1, Z5 and Z6) overlap each other and concordia, and yield a weighted average $^{206}Pb/^{238}U$ age of 471.11 ± 0.35 Ma (MSWD=0.01, probability of fit = 99%; Figure 8), and is interpreted to represent the timing of eruption of this unit.

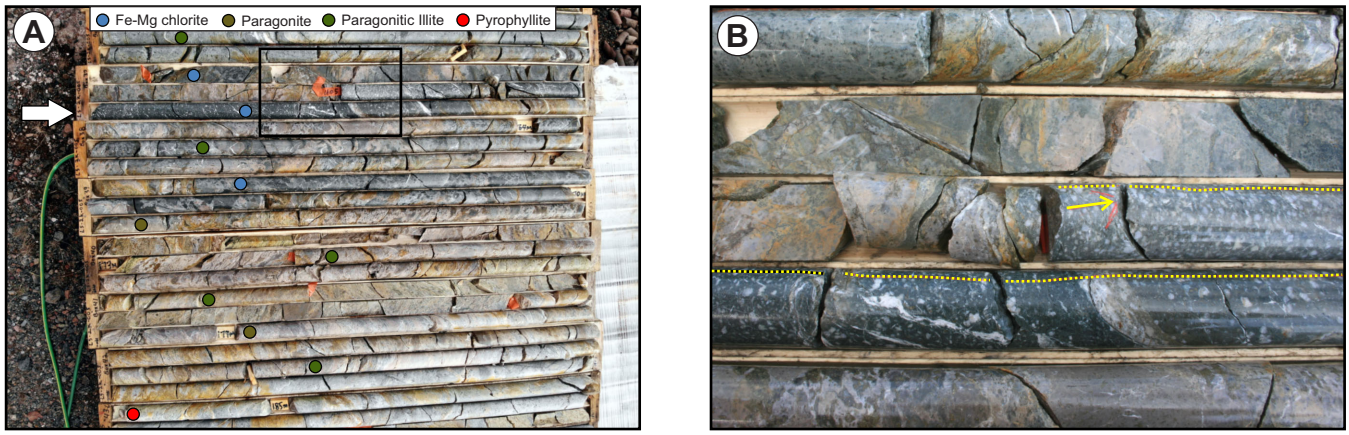

Plate 4. *A) Photograph showing the upper portion of the argillic to advanced argillic alteration zone intersected in DDH LS-2K-005, along with the location and corresponding mineralogy of short wavelength infrared measurements. Note the location of the dated dyke is highlighted by the white arrow; B) Close-up photo (inset box indicated on A) of the upper contact of the post-alteration felsic dyke, intruding paragonite altered polymict lithic breccia.*

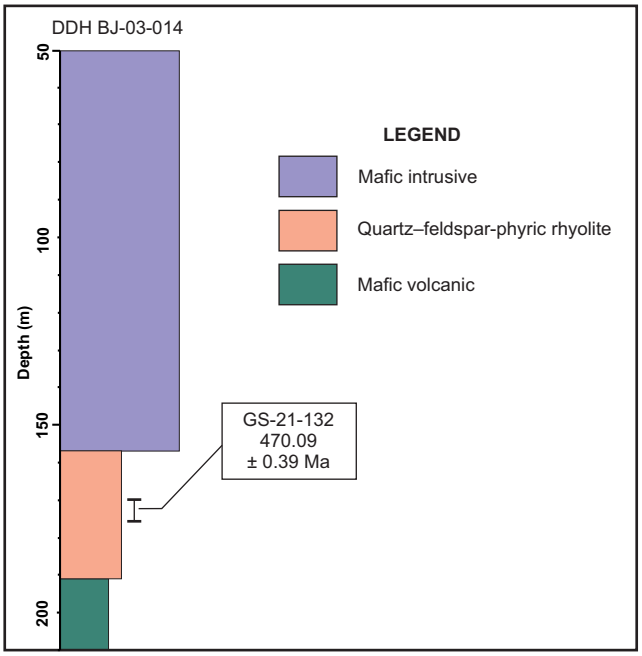

Figure 7. *Partial strip log of DDH BJ-03-014 outlining the distribution of units and the location of the geochronological sample site (GS-21-132).*

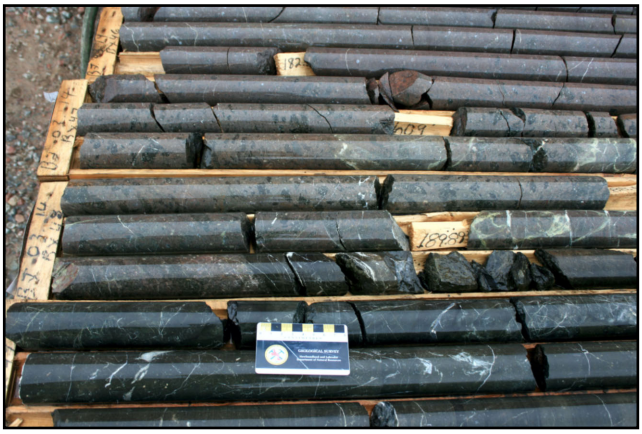

Plate 5. *Photo of the lower contact zone of the quartz–feldspar-phyric rhyolite unit and the underlying fine-grained, locally vesicular, mafic volcanic rocks. Note the development of hyaloclastite within the lower 4 to 5 m of the rhyolite unit; DDH BJ-03-014, 190 m depth.*

The other three analyses are quite discordant with older, inheritance-influenced ages, while the third analysis (Z3) is imprecise and not useful (Figure 8A).

The second sample, GS-21-195, from a coherent rhyolite of the Intermediate Footwall member of the Ski Hill Formation, consists of euhedral feldspar phenocrysts within a fine-grained quartz–feldspar bearing groundmass (Plate 8).

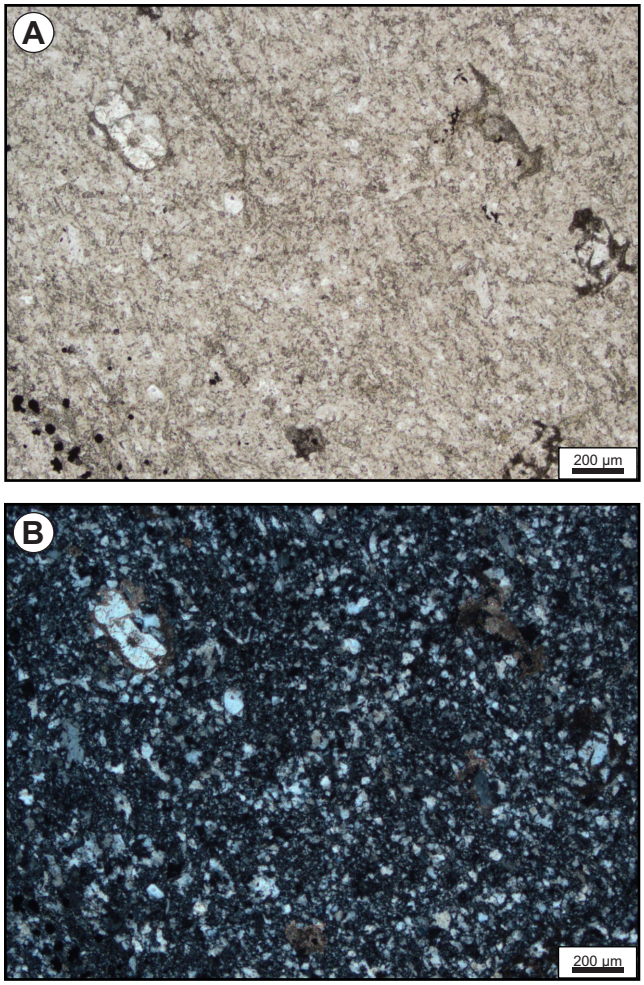

Plate 6. *A) Plane-polarized photomicrograph of sample GS-21-192, illustrating the fine-grained quartz-rich groundmass, which is locally host to rare feldspar phenocrysts and patchy carbonate alteration; B) Cross-polar view of (A).*

Processing of this sample produced a relatively low yield of tiny, pale-yellow zircon subhedra with rare facets (Figure 9). Analyses from this zircon population have produced data that are concordant but continue to reflect an apparent scatter in Pb/U ages, with four of the five analyses yielding $^{206}Pb/^{238}U$ dates between 472.3 ± 1.4 Ma and 469.6 ± 0.6 Ma. The best two youngest analyses from this group yield an average age of approximately 469.7 ± 0.5 Ma, while the oldest two give an age of 471.7 ± 0.6 Ma. A weighted average of all four (Z1, Z3, Z4, Z5) gives an age of 470.4 ± 1.8 Ma, but the fit is poor. Fraction Z2, with a distinctly lower Th/U ratio (Table 2) is more discordant (plotting outside the limits of Figure 9) and likely reflects significant Pb-loss or younger recrystallization. The discordance of fraction Z2 suggests that the younger cluster (Z1 and Z4) may be also affected by minor Pb loss. The current stratigraphic interpre-

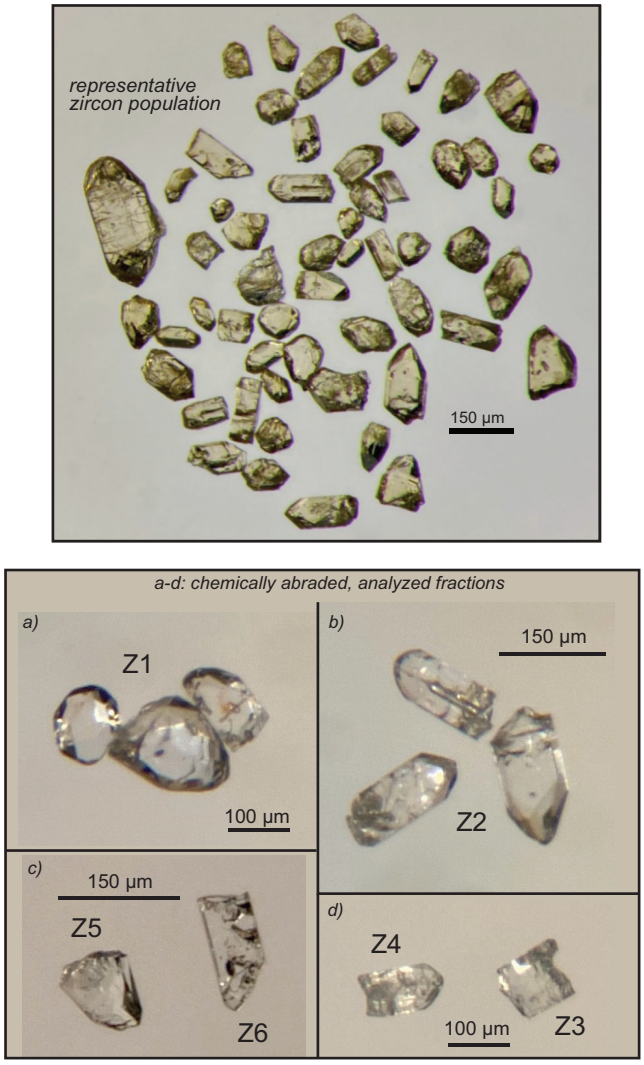

Plate 7. *Representative photographs of the zircon population obtained for Lundberg Hill Formation (sample GS-21-192) along with those grains included within the analyzed fractions.*

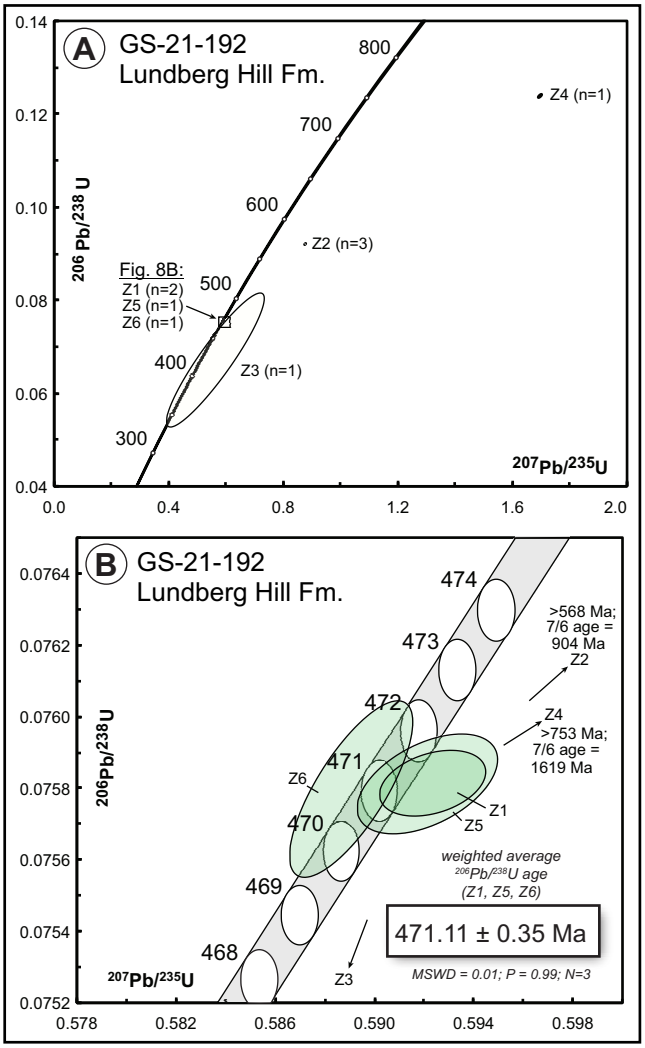

Figure 8. *Concordia diagram of U–Pb results for sample GS-21-192, outlining all analyses (A) and a detailed view of concordant points used in age calculation (B).*

tation of this unit, combined with the age constraints of bounding units (*i.e.*, being younger than sample GS-21-192 and older than sample GS-22-152; *see* Figure 2), suggests the older age of 471.7 ± 0.6 Ma best represents the emplacement age of this unit.

The third sample from the Buchans Group, GS-22-152, represents a sample of the Oriental-Sandfill member of the Buchans River Formation (*cf.* Allen *et al.*, *this volume* and references therein). This unit consists of sub- to anhedral quartz and feldspar phenocrysts supported within a fine-grained, chlorite–phengite dominated groundmass (Plate 9). The quartz phenocrysts display common resorption textures and the feldspar crystals are highly fractured as a result of the fragmented nature of the unit. From this sample four zircon fractions have been analyzed, each of which comprised two grains (Figure 10). Results from these analyses show some spread in Pb/U ages, with $^{206}Pb/^{238}U$ ages ranging from 470.1 to 474.2 Ma. Assuming the spread to older ages reflects minor inheritance, the youngest two fractions, which overlap strongly in terms of $^{206}Pb/^{238}U$ ratios, give a weighted average age of 470.20 ± 0.70 Ma. This is tentatively interpreted as the emplacement age of the synvolcanic intrusion.

The final sample from the Buchans area represents a felsic dyke that intrudes along the Old Buchans Fault (GS-21-194). This unit consists of subhedral feldspar phenocrysts within a quartz–feldspar-rich groundmass (Plate 10). The feldspar phenocrysts display weak to moderate white mica alteration. In total, five analyses were carried out

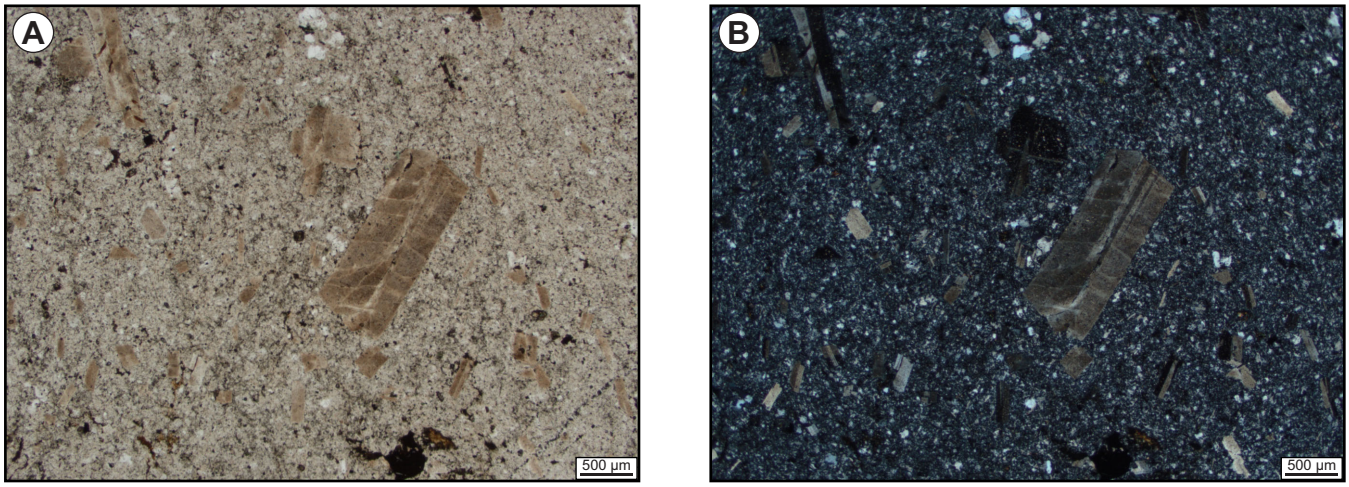

Plate 8. *A) Plane-polarized photomicrograph of sample GS-21-195, illustrating the feldspar-phyric nature of the Intermediate Footwall member; B) Cross-polar view of (A).*

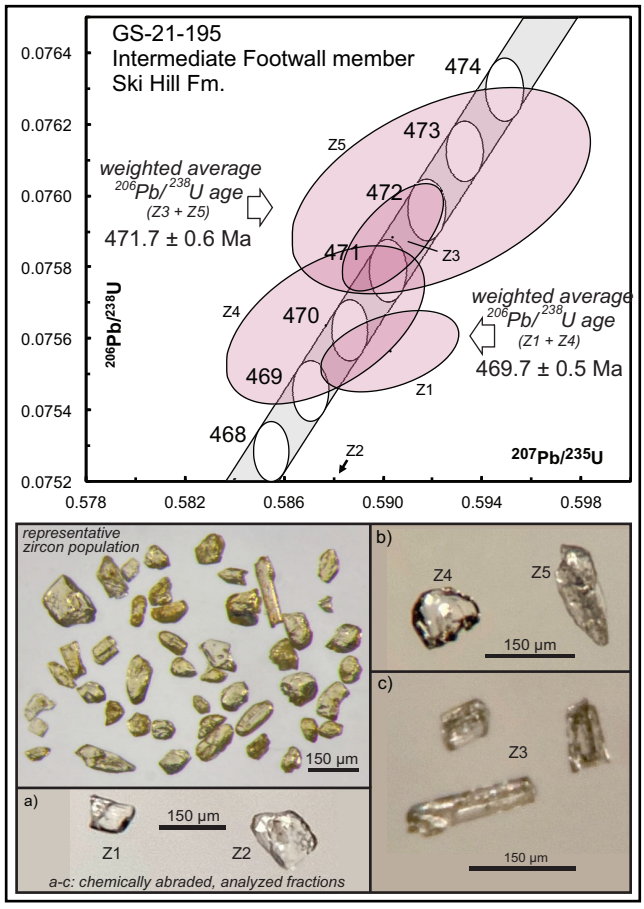

Figure 9. *Concordia diagram of U–Pb results for sample GS-21-195, outlining the distribution of the four concordant analyses, along with representative photos of the recovered zircon crystals and those included in individual analysis.*

on zircon fractions from this rhyolite, with each fraction representing between 2–3 zircon grains each (Figure 11). The results all show very good concordance, although there is some spread in terms of Pb/U ages. However, with the exception of fraction Z1 (with comparatively higher Th/U, and $^{206}Pb/^{238}U$ age = 454.6 Ma; Table 2), there is good overlap between the remaining analyses which yield $^{206}Pb/^{238}U$ ages between ~450.0 and 451.9 Ma. A weighted average age calculated for the two youngest analyses, Z3 and Z4 are in good agreement yielding an average $^{206}Pb/^{238}U$ age of 450.32 ± 0.68 Ma. This age is interpreted as the best estimate of the crystallization age of the dyke.

TOWER PROSPECT

The rhyolitic dyke crosscutting a zone of hydrothermal alteration in the area of the Tower prospect consists of anhedral to subhedral quartz and feldspar phenocrysts within a fine-grained chlorite-rich groundmass (Plate 11). Four zircon fractions were analyzed from this porphyry dyke (GS-21-110). The resultant data points are all concordant and mostly show good, consistent overlap (Figure 12). The best fit weighted average $^{206}Pb/^{238}U$ age comes from a weighted average of analyses Z1, Z2 and Z4, yielding an age of 467.51 ± 0.44 Ma (MSWD = 0.05; 95% probability of fit). Assuming that these zircons are magmatic and do not reflect inheritance from assimilated material, this age is inferred to represent the emplacement age of the dyke.

MARY MARCH BROOK AREA

The sample from the felsic volcanic unit collected east of Mary March brook consists of sub- to euhedral feldspar in a fine-grained quartz–feldspar-bearing, chloritic ground-

Table 2. U–Pb chemical abrasion isotope dilution TIMS data for zircon analyses from the Buchans area, Newfoundland

Sample Fractions	$Pb^{T/a}$ Pb_C	Pb_C[b] (pg)	U (ppm)	Th/[c] U	Isotope Ratios								Ages (Ma)					
					$^{206}Pb/^{204}Pb$[d]	$^{207}Pb/^{235}U$[e]	2σ	$^{206}Pb/^{238}U$[e]	2σ	Corr.[f] Coef.	$^{207}Pb/^{206}Pb$	2σ	$^{207}Pb/^{206}Pb$	2σ	$^{207}Pb/^{235}U$	2σ	$^{206}Pb/^{238}U$	2σ
GS-21-132; Qz-Fsp-phyric rhyolite, Mary March Brook area																		
Z1 (1)	31.5	0.28	106	0.71	1862	0.589525	0.001766	0.075640	0.000074	0.515	0.05653	0.00015	473.1	5.8	470.56	1.13	470.04	0.45
Z2 (1)	22.2	0.34	129	0.77	1302	0.589472	0.004074	0.075660	0.000171	0.441	0.05650	0.00036	472.0	14.0	470.53	2.60	470.17	1.03
Z3 (3)	307.2	0.47	409	1.35	15563	0.588923	0.002542	0.075650	0.000303	0.949	0.05646	0.00008	470.5	3.0	470.18	1.62	470.11	1.81
Z4 (2)	78.1	0.62	295	0.63	4679	0.590225	0.003162	0.075779	0.000381	0.950	0.05649	0.00009	471.6	3.7	471.01	2.02	470.88	2.28
GS-21-192; Lundberg Hill Fm., Buchans area																		
Z1 (2)	22.9	2.18	209	0.72	1356	0.592346	0.001751	0.075819	0.000074	0.345	0.05666	0.00016	478.4	6.1	472.36	1.12	471.12	0.45
Z2 (3)	108.0	0.66	353	0.67	6360	0.879124	0.001467	0.092183	0.000107	0.822	0.06917	0.00007	903.7	2.0	640.51	0.79	568.44	0.63
Z3 (1)	21.2	1.58	448	0.74	1242	0.563001	0.140416	0.067530	0.011664	0.917	0.06047	0.00662	620.3	227.9	453.48	90.67	421.25	70.54
Z4 (1)	51.3	0.40	156	0.43	3153	1.703510	0.005963	0.123867	0.000322	0.796	0.09974	0.00021	1619.3	4.0	1009.85	2.24	752.78	1.85
Z5 (1)	21.5	0.62	162	0.66	1294	0.592131	0.002313	0.075818	0.000113	0.487	0.05664	0.00019	477.7	7.6	472.23	1.47	471.11	0.68
Z6 (1)	47.0	0.50	286	0.70	2782	0.589050	0.002023	0.075803	0.000199	0.759	0.05636	0.00013	466.5	5.0	470.26	1.29	471.03	1.19
GS-21-195; Intermediate Footwall member, Ski Hill Fm.																		
Z1 (1)	31.9	0.51	188	0.88	1811	0.590257	0.002278	0.075571	0.000092	0.418	0.05665	0.00020	477.9	7.8	471.03	1.45	469.63	0.55
Z2 (1)	17.0	1.46	229	0.54	1057	0.527892	0.002009	0.068898	0.000071	0.412	0.05557	0.00019	435.2	7.8	430.41	1.34	429.51	0.43
Z3 (3)	47.0	0.39	172	0.81	2705	0.590378	0.001674	0.075888	0.000122	0.650	0.05642	0.00012	469.1	4.8	471.11	1.07	471.53	0.73
Z4 (1)	16.9	0.67	136	0.72	1005	0.587627	0.003296	0.075643	0.000180	0.513	0.05634	0.00027	465.9	10.7	469.35	2.11	470.07	1.08
Z5 (1)	14.2	0.54	190	0.79	834	0.592319	0.004951	0.076017	0.000235	0.472	0.05651	0.00042	472.5	16.4	472.35	3.16	472.31	1.41
GS-21-194; Fsp-phyric rhyolite dyke																		
Z1 (2)	30.0	0.67	552	0.32	1958	0.564272	0.001413	0.073064	0.000070	0.438	0.05601	0.00013	452.9	5.0	454.30	0.92	454.59	0.42
Z2 (2)	44.1	0.54	587	0.15	3008	0.560405	0.001573	0.072613	0.000157	0.814	0.05597	0.00009	451.3	3.6	451.79	1.02	451.88	0.94
Z3 (2)	21.4	1.16	360	0.16	1463	0.558478	0.001937	0.072404	0.000153	0.681	0.05594	0.00014	450.1	5.7	450.54	1.26	450.62	0.92
Z4 (3)	17.4	0.93	335	0.16	1196	0.557370	0.002341	0.072288	0.000173	0.613	0.05592	0.00019	449.2	7.4	449.81	1.53	449.93	1.04
Z5 (3)	25.0	0.75	272	0.19	1700	0.559627	0.001981	0.072508	0.000136	0.609	0.05598	0.00016	451.5	6.3	451.28	1.29	451.25	0.82
GS-22-110; Qz-fsp rhyolite porphyry dyke																		
Z1 (1)	23.3	0.63	360	0.68	1391	0.584574	0.002055	0.075206	0.000135	0.558	0.05638	0.00016	467.2	6.5	467.40	1.32	467.44	0.81
Z2 (1)	6.9	1.76	299	0.66	429	0.584875	0.005430	0.075242	0.000190	0.398	0.05638	0.00048	467.2	19.1	467.59	3.48	467.66	1.14
Z3 (1)	81.3	0.62	326	0.45	5099	0.586402	0.001289	0.075391	0.000121	0.831	0.05641	0.00007	468.6	2.8	468.57	0.82	468.56	0.73
Z4 (2)	15.9	1.52	290	0.74	941	0.584578	0.002463	0.075217	0.000104	0.319	0.05637	0.00023	466.8	8.8	467.40	1.58	467.51	0.62
GS-22-152; Oriental-Sandfill member, Buchans River Fm.																		
Z1 (2)	29.3	0.72	257	0.67	1752	0.587968	0.002119	0.075708	0.000198	0.745	0.05633	0.00014	465.2	5.3	469.57	1.36	470.46	1.19
Z2 (2)	17.5	1.02	105	0.77	1026	0.595122	0.002377	0.076334	0.000104	0.410	0.05654	0.00021	473.8	8.1	474.13	1.51	474.21	0.62
Z3 (2)	25.3	0.67	101	0.77	1478	0.591624	0.002361	0.075961	0.000187	0.676	0.05649	0.00017	471.6	6.5	471.90	1.51	471.97	1.12
Z4 (2)	24.9	1.07	159	0.72	1470	0.589204	0.002103	0.075640	0.000150	0.625	0.05650	0.00016	471.9	6.2	470.36	1.34	470.05	0.90

Notes: Zircon grains were chemically abraded (CA) (Mattinson, 2005), and dissolutions spiked with the EarthTime $^{205}Pb/^{233}U/^{235}U$ tracer. Errors are 2σ absolute. Ages calculated using the U decay constants of Jaffey *et al.* (1971): λ235 = 9.8485E-10/y and λ238 = 1.55125E-10/y. (#) - number of grains in analyzed fraction. Correction for initial ^{230}Th disequilibrium in $^{206}Pb/^{238}U$ and $^{207}Pb/^{206}Pb$ assumes $Th/U_{[magma]}$ = 4.2. A $^{238}U/^{235}U$ ratio of 137.88 was used for model age calculations.

[a] Ratio of total Pb in the analysis (radiogenic + common) to total common Pb.

[b] Total common Pb (in picograms); assumed isotopic composition of laboratory blank ($^{206}Pb/^{204}Pb$ = 18.49 ± 0.4%; $^{207}Pb/^{204}Pb$ = 15.59 ± 0.4%; $^{208}Pb/^{204}Pb$ = 39.36 ± 0.4%)

[c] Th/U calculated from radiogenic $^{208}Pb/^{206}Pb$ ratio and $^{207}Pb/^{206}Pb$ age, assuming concordance.

[d] $^{206}Pb/^{204}Pb$ corrected for fractionation and common Pb in the spike.

[e] Pb/U ratios corrected for fractionation, common Pb in the spike, and blank.

[f] Corr. Coef. is the correlation coefficient for Concordia plot X-Y errors.

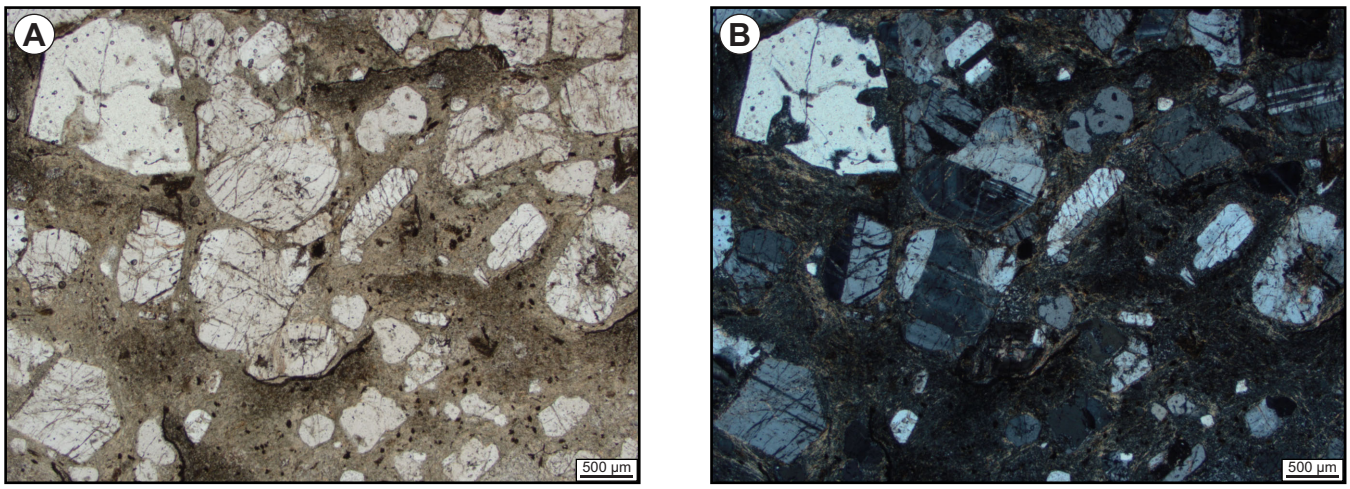

Plate 9. *A) Plane-polarized photomicrograph of sample GS-22-152. Note the resorption textures developed within the quartz phenocrysts, which is a common feature of rhyolite units of the Buchans River Formation, and the highly fractured nature of the feldspar crystals within the* in situ *hyaloclastite unit; B) Cross-polar view of (A).*

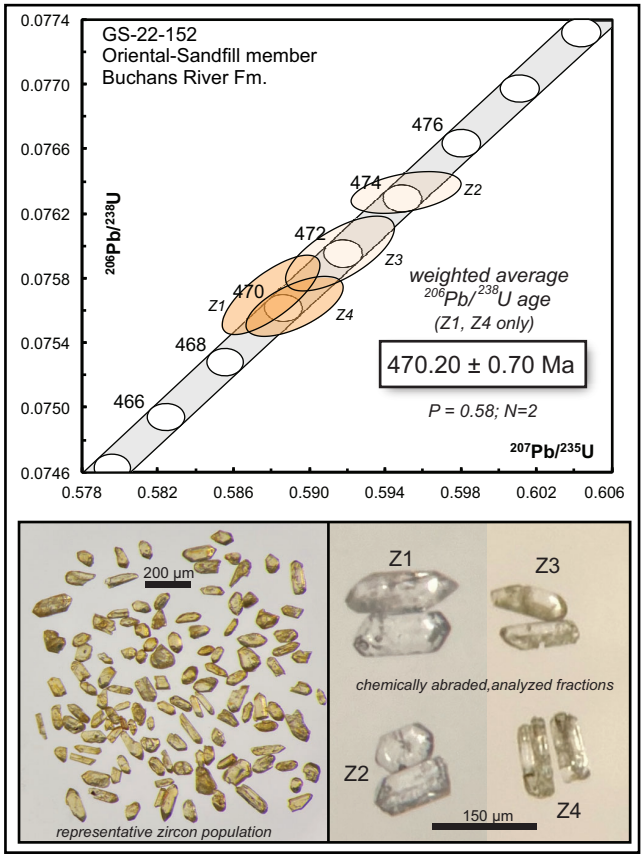

Figure 10. *Concordia diagram of U–Pb results for sample GS-22-152, outlining the distribution of the four concordant analyses, along with representative photos of the recovered zircon crystals and those included in individual analysis.*

mass (Plate 12). This sample (GS-21-132) contained abundant, fine, pale-yellow zircon with a good subpopulation of sharply prismatic grains. Four fractions were analyzed, which produced concordant and overlapping data points (Figure 13). The combined results for all fractions yield a weighted average $^{206}Pb/^{238}U$ age age of 470.09 ± 0.39 Ma (MSWD=0.18, prob. of fit = 91%). and is interpreted as the eruption age for this unit.

DISCUSSION

The U–Pb dating of select units within the recently modified Buchans Group stratigraphy illustrates that the *ca.* 470 Ma volcanism reported in Sparkes *et al.* (2021) is more widespread than first envisaged. Rocks of this age span the Lundberg Hill, Ski Hill and Buchans River formations, demonstrating a period of rapid deposition within an active volcanic environment, which was accompanied by the local development of hydrothermal systems and accompanying VMS mineralization. The re-introduction of the Intermediate Footwall member and recognition of the upper and lower members of the Buchans River Formation highlight the development of VMS mineralization in the Buchans camp, with the onset of mineralization marked by the deposition of the Intermediate Footwall member of the Ski Hill Formation (Allen *et al.*, *this volume* and references therein). Units within the lower Buchans River Formation are bound by ore-clast bearing horizons, demonstrating its deposition, at least locally, is essentially coeval with the formation of VMS mineralization. Thus, the age of 470.20 ± 0.70 Ma from the lower Buchans River Formation provides the best approximation for the age of VMS mineralization

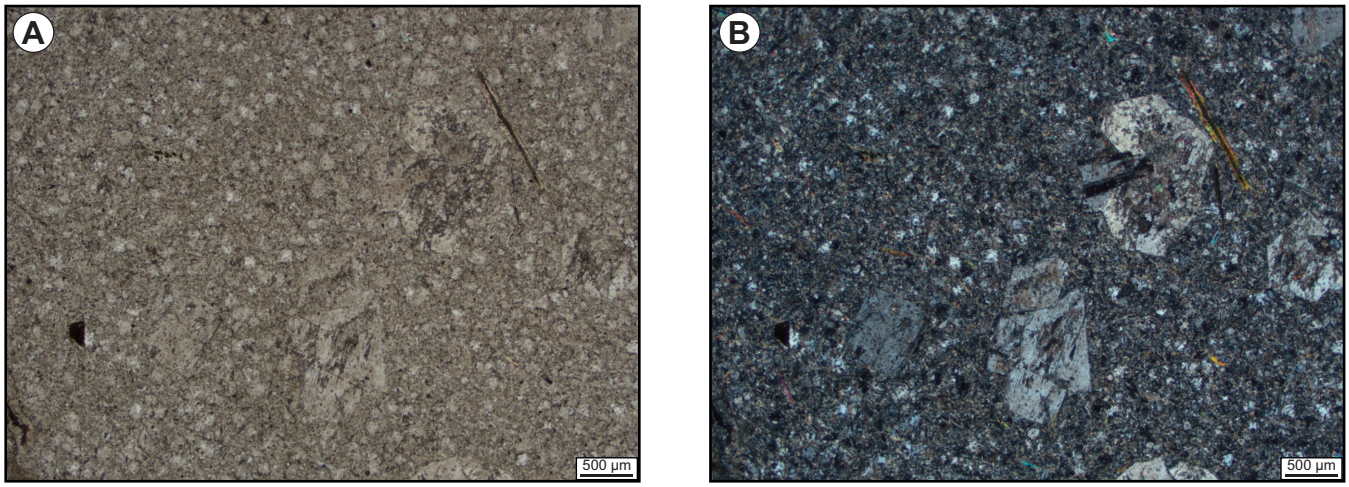

Plate 10. *A) Plane-polarized photomicrograph of sample GS-21-194, illustrating the feldspar-phyric nature of the rhyolite dyke; B) Cross-polar view of (A).*

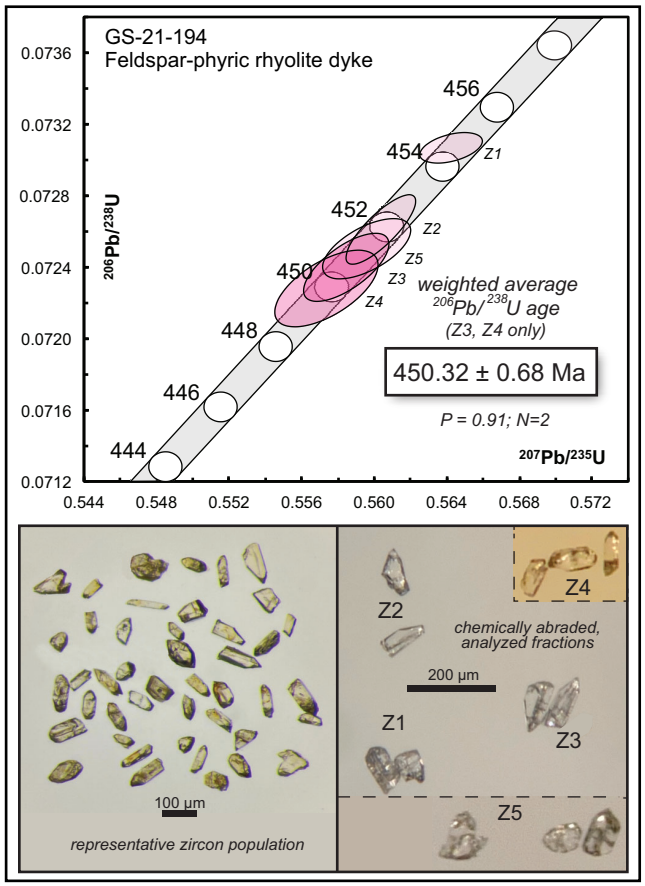

Figure 11. *Concordia diagram of U–Pb results for sample GS-21-194, outlining the distribution of the five concordant analyses, along with representative photos of the recovered zircon crystals and those included in individual analysis.*

within the Buchans camp, based on current stratigraphic interpretations and geochronological constraints.

This is further supported by the minimum age constraint of 467.51 ± 0.44 Ma from the felsic dyke crosscutting argillic to advanced argillic alteration in the area of the Tower prospect. Elsewhere in the region, similar alteration zones are demonstrated to be associated with the development of VMS mineralization (Sparkes and Hinchey, 2023). Although no massive sulphide mineralization has yet been identified within the Tower alteration zone, it is situated along strike from similar alteration (*e.g.*, Powerhouse prospect; *cf.* Allen *et al.*, *this volume*), which is more proximal to the main Buchans ore bodies. Current interpretations of the Tower prospect suggest that it represents a similar stratigraphic setting to the Buchans River Formation and thus the minimum age constraint for the hydrothermal alteration is equally applicable to the mineralization within the main Buchans camp. Thus, based on current age constraints, hydrothermal activity within the Buchans camp can be bracketed between 472.3–467.07 Ma, constraining the mineralization to within a period of some 5.2 Ma.

Thrusting and the related structural dismemberment of the Buchans deposits has until now been poorly constrained and largely based on the absolute ages of rocks occurring within the footwall and hangingwall zones of regional-scale structures (Kirkham, 1987). The Old Buchans Fault, which represents the floor thrust to a major structural panel within the Buchans camp is also related to the development of these regional-scale structures (Calon and Green, 1987). The age from a felsic dyke intruding along the Old Buchans Fault, dated at 450.32 ± 0.68 Ma, demonstrates that thrust faulting within the area was already initiated by the Late Ordovician.

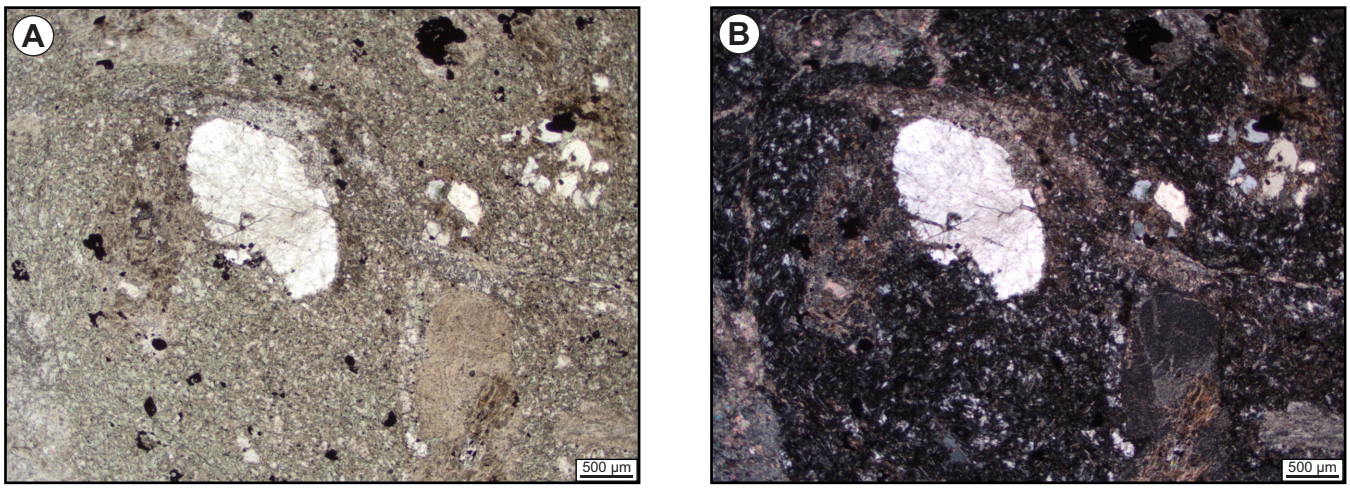

Plate 11. *A) Plane-polarized photomicrograph of sample GS-21-110, outlining the nature of the quartz and feldspar phenocrysts contained within a chlorite-rich groundmass, which contrasts that of the white-mica dominated alteration in the adjacent country rock; B) Cross-polar view of (A).*

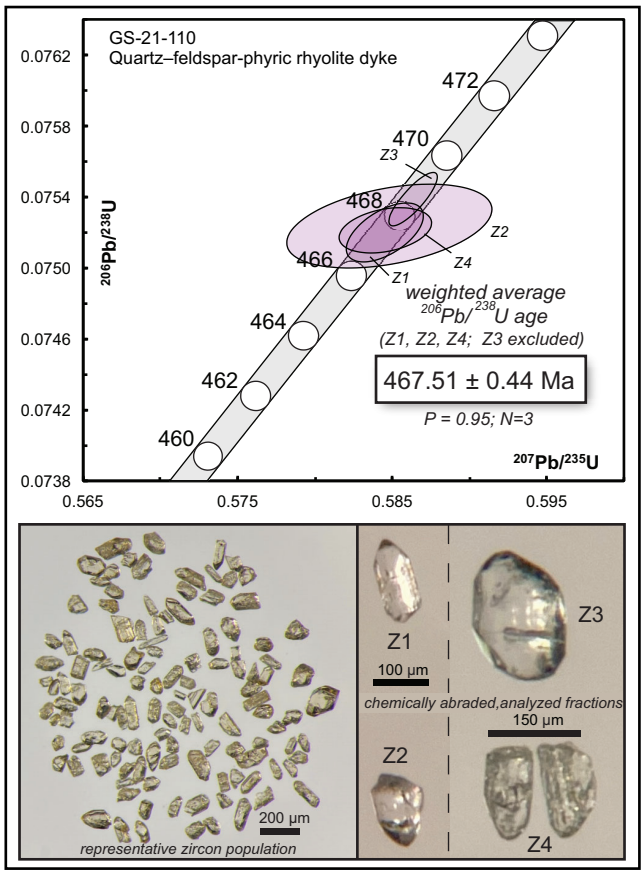

Figure 12. *Concordia diagram of U–Pb results for sample GS-21-110, outlining the distribution of the four concordant analyses, along with representative photos of the recovered zircon crystals and those included in individual analysis.*

Thus, the onset of deformation in the region can now be bracketed between 470.9–449.64 Ma.

Prior to the ages reported here, the bulk of the geochronological data for the Buchans area has been generated through SHRIMP analysis (*cf.* Figure 5 of Sparkes *et al.* (2021) and references therein). The direct sampling of an outcrop previously dated using SHRIMP has shown some discrepancy between these two techniques, with the SHRIMP age of 465 ± 4 Ma (RAX05913; z8774; Zagorevski *et al.*, 2016) *vs.* the CA-ID-TIMS age of 471.7 ± 0.6 Ma (GS-21-195). If the alternative age of 469.7 ± 0.5 Ma is considered for sample GS-21-195 (*see* above), results from these two techniques are close to overlapping within analytical error. However, the SHRIMP data may potentially reflect slightly younger ages due to the effects of minor unresolved lead-loss, which is less of an issue with CA-ID-TIMS due to the sample pretreatment procedure. In any case, there no longer appears to be supporting evidence for the presence of an older arc sequence underlying the Buchans Group, as previously implied by Zagorevski *et al.* (2015) and Sparkes *et al.* (2021).

These and other regional discrepancies, such as the inclusion of rocks correlated with the dated 471.11 ± 0.35 Ma Lundberg Hill Formation within the regional Mary March Brook group by Zagorevski *et al.* (2016; *cf.* Allen *et al.*, *this volume*), which is locally dated at 461.5 ± 4 Ma (Zagorevski *et al.*, 2016), suggest some modifications to regional map units is required within the Buchans area. Likewise, felsic volcanic rocks herein dated at 470.09 ± 0.39 Ma from the area east of Mary March brook have been correlated with both the Red Indian Lake group (Zagorevski *et*

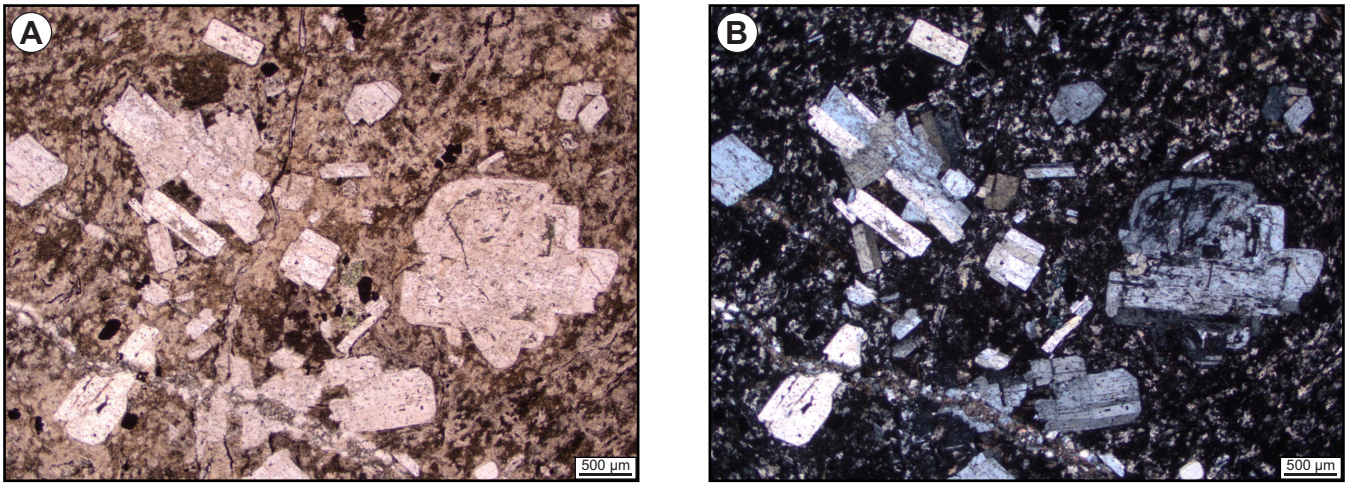

Plate 12. *A) Plane-polarized photomicrograph of sample GS-21-132, which contains sub- to euhedral feldspars and lesser quartz in a fine-grained, chloritic groundmass; B) Cross-polar view of (A).*

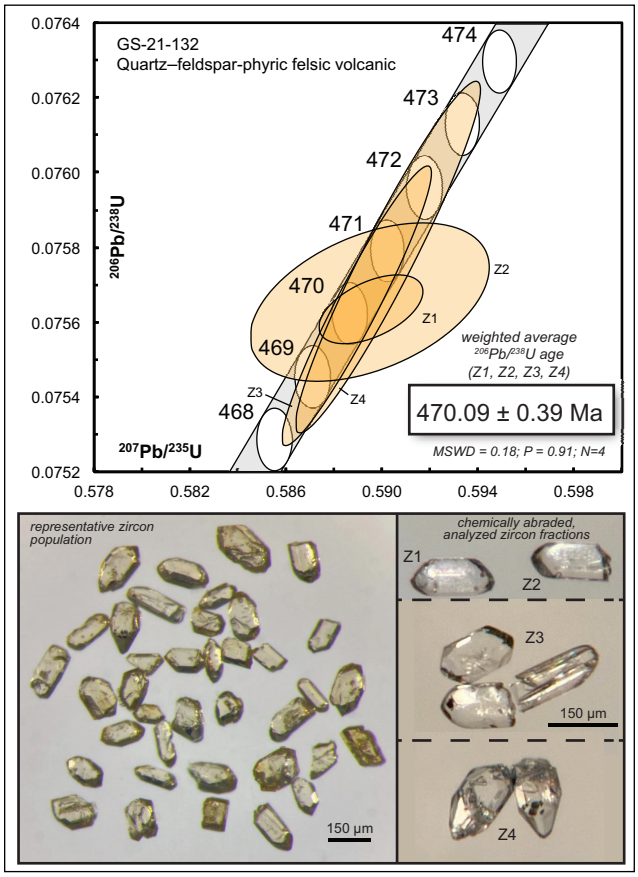

Figure 13. *Concordia diagram of U–Pb results for sample GS-21-132, outlining the distribution of the four concordant analyses, along with representative photos of the recovered zircon crystals and those included in individual analysis.*

al., 2016), as well as the Gullbridge structural tract (O'Brien, 2009; *cf.* Sparkes *et al.*, 2021). To fully evaluate these and other regional inconsistencies, additional CA-ID-TIMS dating is required to better define the distribution of key units within the southern BRAB.

CONCLUSION

The geochronological sampling of units within the Buchans Group stratigraphy, in part identified through the detailed core logging conducted by Buchans Minerals personnel, has provided important age constraints on the development of the group, as well as the associated VMS mineralization. These data bracket the main period of hydrothermal activity in the region as well as the overprinting structural features. This new information allows for a more accurate comparison of these significant events with the development of similar features along the length of the Buchans-Roberts Arm Belt. In addition, these new absolute age constraints for the Buchans Group provide a foundation for future studies in the region, and will aid in the expansion of this geological framework, beyond the limits of the immediate Buchans area.

ACKNOWLEDGMENTS

Paul Moore, David Butler and Marina Schofield are thanked for providing assistance in the sample selection of key units collected in the Buchans area. William Oldford and Derrick Keats are gratefully acknowledged for assistance in the Buchans core library.

REFERENCES

Allen, R. and Schofield, M.
2023: Volcanic facies, lithogeochemistry and vectors to ore at Buchans massive sulphide camp, Newfoundland. Stage 1 Final Report. Unpublished internal company report prepared for Buchans Minerals Resources.

Allen, R.L., Schofield, M. and Sparkes, G.W.
This volume: Volcanic facies mapping and related hydrothermal alteration studies of the Buchans Camp, southern Buchans–Roberts Arm belt, central Newfoundland.

Calon, T.J. and Green, F.K.
1987: Preliminary results of a detailed structural analysis of the Buchans mine area. *In* Buchans Geology, Newfoundland. *Edited by* R.V. Kirkham. Geological Survey of Canada, Paper 86-24, pages 273-288.

Hamilton, M.A., Álvaro, J.J., Barr, S.M., Jensen, S., Johnson, S.C., Palacios, T., van Rooyen, D. and White, C.E.
2023: U-Pb zircon ages from tuffaceous beds in the Terreneuvian to Cambrian Series 2 sections of southern New Brunswick, Canada: New constraints on chronostratigraphic correlations and the Cambrian time scale. *In* Supercontinents, Orogenesis and Magmatism. Geological Society, London, Special Publications, Volume 542. https://doi.org/10.1144/SP542-2022-11.

Jaffey, A.H, Flynn, K.F. Glendenin, L.E., Bentley, W.C. and Essling, A.M.
1971: Precision measurement of the half-lives and specific activities of ^{235}U and ^{238}U. Physical Review, Section C, Nuclear Physics, Volume 4, pages 1889-1906.

Kirkham, R.V.
1987: Tectonic setting of the Buchans Group. In Buchans Geology, Newfoundland. Edited by R.V. Kirkham. Geological Survey of Canada, Paper 86-24, pages 23-34.

Mattinson, J.M.
2005: Zircon U–Pb chemical abrasion (CA-TIMS) method; combined annealing and multi-step partial dissolution analysis for improved precision and accuracy of zircon ages. Chemical Geology, Volume 220, pages 47-66.

O'Brien, B.H.
2009: Geology of the Little Joe Glodes Pond–Catamaran Brook region with emphasis on the Robert's Arm volcanic belt (parts of NTS 12H/1 and 12A/16), west-central Newfoundland. Map 2009-28. Government of Newfoundland and Labrador, Department of Natural Resources, Geological Survey, Open File NFLD/3053.

Saunders, P., Harris, J. and Woods, D. V.
2000: Assessment report on geophysical and diamond drilling exploration for 2000 submission for fee simple grants volume 1 folios 61-62 and the Anglo-Newfoundland Development Company Limited Charter and for second year and second year supplementary to sixth year supplementary assessment for licence 4548 on claim 16507, licence 4793 on claims 16420-16421 and licences 5651M, 6192M, 6303M-6307M, 6429M and 7219M-7223M on claims in the Little Sandy Lake area, near Buchans, central Newfoundland, 3 reports. Newfoundland and Labrador Geological Survey, Assessment File 12A/15/0991, 244 pages.

Sparkes, G.W.
2022: Short wavelength infrared spectrometry studies of sericitic alteration zones, southern Buchans–Roberts Arm Belt, Newfoundland. *In* Current Research. Government of Newfoundland and Labrador, Department of Industry, Energy and Technology, Geological Survey, Report 22-1, 34 pages.

Sparkes, G.W., Hamilton, M.A. and Dunning, G.R.
2021: Age constraints on VMS mineralization, central Buchans–Roberts Arm Belt, Newfoundland. *In* Current Research. Government of Newfoundland and Labrador, Department of Industry, Energy and Technology, Geological Survey, Report 21-1, 16 pages.

Sparkes, G.W. and Hinchey, J.G.
2023: White mica zonation patterns associated with hybrid bimodal-felsic VMS systems: Examples from the Tulks Volcanic and Buchans–Roberts Arm belts, central Newfoundland. In Current Research. Government of Newfoundland and Labrador, Department of Industry, Energy and Technology, Geological Survey, Report 23-1, 27 pages.

Swinden, H.S., Jenner, G.A. and Szybinski, Z.A.
1997: Magmatic and tectonic evolution of the Cambrian–Ordovician margin of Iapetus: geochemical and isotopic constraints from the Notre Dame Subzone, Newfoundland. *In* Nature of Magmatism in the Appalachian Orogen. *Edited by* A.K. Sinha, J.B. Whalen and J.P. Hogan. Geological Society of America, Memoir 191, pages 337-365.

Thurlow, J.G., Spencer, C.P., Boerner, D.E., Reed, L.E. and Wright, J.A.
1992: Geological interpretation of a high resolution reflection seismic survey at the Buchans mine, Newfoundland. Canadian Journal of Earth Sciences, Volume 29, pages. 2022-2037.

Thurlow, J.G. and Swanson, E.A.
1987: Stratigraphy and structure of the Buchans Group. In Buchans Geology, Newfoundland. *Edited by* R.V. Kirkham. Geological Survey of Canada, Paper 86-24, pages 35-46.

Whalen, J.B., Currie, K.L. and van Breemen, O.
1987: Episodic Ordovician–Silurian plutonism in the Topsails igneous terrane, western Newfoundland. Transactions of the Royal Society of Edinburgh: Earth Sciences, Volume 78, pages 17-28.

Whalen, J., Zagorevski, A., McNicoll, V.J. and Rogers, N.
2013: Geochemistry, U–Pb geochronology, and genesis of granitoid clasts in transported volcanogenic massive sulfide ore deposits, Buchans, Newfoundland. Canadian Journal of Earth Sciences, Volume 50, pages. 1116-1133.

2009: Geochemical characteristics of the Ordovician volcano-sedimentary rocks in the Mary March Brook area. *In* Current Research. Government of Newfoundland and Labrador, Department of Natural Resources, Geological Survey, Report 9-1, pages 271-288.

Zagorevski, A., McNicoll, V.J., Rogers, N. and van Hees, G.H.
2016: Middle Ordovician disorganized arc rifting in the peri-Laurentian Newfoundland Appalachians: Implications for evolution of intra-oceanic arc systems. Journal of the Geological Society, Volume 173, pages 76-93.

Zagorevski, A., McNicoll, V., van Staal, C.R., Kerr, A. and Joyce, N.
2015: From large zones to small terranes to detailed reconstruction of an Early to Middle Ordovician arc-backarc system preserved along the Iapetus suture zone: A legacy of Hank Williams. Geoscience Canada, Volume 42, pages 125-150.

Zagorevski, A., McNicoll, V.J., van Staal, C.R. and Rogers, N.
2007: Tectonic history of the Buchans Group; evidence for late Taconic accretion of a peri- Laurentian arc terrane and its reimbrication during the Salinic Orogeny. Geological Society of America, Abstracts with Programs, Volume 39, page 51.

Zagorevski, A. and Rogers, N.
2008: Stratigraphy and structural geology of the Ordovician volcano-sedimentary rocks in the Mary March Brook area. *In* Current Research. Government of Newfoundland and Labrador, Department of Natural Resources, Geological Survey, Report 8-1, pages 101-113.

Zagorevski, A., Rogers, N., van Staal, C.R., McNicoll, V., Lissenberg, C.J. and Valverde-Vaquero, P.
2006: Lower to Middle Ordovician evolution of peri-Laurentian arc and backarc complexes in Iapetus; constraints from the Annieopsquotch accretionary tract, central Newfoundland. Geological Society of America Bulletin, Volume 118, pages 324-342.